Kinetics of Oxidation of a Hemicellulose Model Compound by Chlorine Dioxide in Bleaching

Shuangquan Yao,[a,b] Chengqi Feng,[a,b] Cheng Wang,[a,b] Baojie Liu,[a,b] Lingzhi Huang,[a,b] Shuangxi Nie,[a,b] Tianyi Zhang,[c] and Chengrong Qin [a,b,*]

Kinetics of the oxidation of D-xylose, a hemicellulose model compound, by chlorine dioxide was studied under simulated bleaching conditions. The final reaction product, chloroacetic acid, which is a type of adsorbable organic halogen (AOX), was detected by gas chromatography-mass spectrometer (GC-MS). The kinetic equation was expressed as $dW/dt = 2.36e^{-560/T}[H^+]^{0.05}[ClO_2]^{0.11}X^{0.92}$. The reaction exhibited first-order kinetics, with a good agreement between the experimental and modelling data. The reaction activation energy was 4.66 $kJ.mol^{-1}$. Thus, the process is not controlled by a chemical reaction, but rather, it is controlled by hemicellulose properties. These results might have potential for resolving the major problems of environmental pollution in elemental chlorine-free (ECF) bleaching of pulp.

Keywords: AOX; Hemicellulose model compounds; GC-MS; Oxidation kinetics; Chlorine dioxide

*Contact information: a: Department of Light Industrial and Food Engineering, Guangxi University, Nanning, 530004, PR China; b: Guangxi Key Laboratory of Clean Pulp & Papermaking and Pollution Control, Nanning 530004, PR China; c: St. Louis University High School, St. Louis, MO 63110, USA; * Corresponding author: qin_chengrong@sina.com*

INTRODUCTION

There is considerable interest and public concern regarding the discharge of pulp bleaching effluents to the environment because they contain high amounts of chlorinated organics originating from elemental chlorine bleaching treatments (Bouiri and Amrani 2010; Li *et al.* 2016; Saelee *et al.* 2016). One important group of substances is organic halogens, which are characterized by toxicity and bioaccumulation (Jaacks and Staimez 2015; Yeh *et al.* 2014; Wang *et al.* 2014). The total concentration of organic halogens is mostly due to adsorbable organic halogen (AOX) (Nie *et al.* 2015; Yao *et al.* 2017). This is an estimate of the soluble and organically bound chlorine in pulp bleaching effluents (Hart and Santos 2013; Fang *et al.* 2016). Pulping processes utilize large amounts of water, and elemental chlorine is still in use in some of the paper pulp producing plants due to the superior quality of the paper produced and the cost effectiveness of chlorine bleaching (Nie Shuangxi *et al.* 2014). For the above reasons, AOX reduction technology has become an advanced research hotspot (Singh *et al.* 2008; Bouiri and Amrani 2010).

To meet increasingly stringent discharge limits, the amount of AOX discharged from pulp mills can be reduced in two ways: optimization of the mill process and adoption of technologically advanced treatment systems. Optimization of mill processes includes lowering the pulp concentration, extending the cooking time, oxygen delignification and increasing chlorine dioxide substitution, changing the pH in the First Chlorine Dioxide Bleaching Stage (D_0) (initial pH 2 to 4, final pH 8 to 9), and reducing the chlorine dosage during bleaching as well as subsequent AOX discharges from the

bleach plant (Baycan *et al.* 2007; Benattar *et al.* 2007; Hart and Connell 2008). External treatments, such as biological treatments, reduce AOX discharge from the mill to the receiving water. Xylanase (Dai *et al.* 2016) and laccase (Pei *et al.* 2016) have been evaluated in elemental chlorine free (ECF) bleaching of eucalyptus kraft pulp, resulting in a 34% reduction of AOX in the effluents (Sharma *et al.* 2014). Xylanase pre-treatment removes HexA and exposes more lignin, decreasing the chlorine dioxide demand, thus reducing the concentration of AOX (Nie *et al.* 2015; 2018). An external chemical treatment has been developed that significantly reduces AOX in bleach plant effluent prior to biological treatment. The inclusion of additives, such as dimethyl sulfoxide (DMSO) (Joncourt *et al.* 2000), hydrogen peroxide (Baycan *et al.* 2007), or amino sulfonic acid (Yoon and Wang 2002), can be considered. For the portion of the lignin that is removed, alkali extraction is an effective method to reduce AOX concentration.

Furthermore, hemicellulose affects AOX formation. A pH pre-corrected hot water pre-treatment has been developed (Yao *et al.* 2015; 2017). The influence of lignin on AOX concentration is eliminated by controlling the hot water extraction time. Consequently, the AOX concentration is decreased by 33.3% under the optimal hot water extraction conditions. The main monosaccharides in hemicellulose are D-xylose, L-arabinose, D-glucose, D-galactose, and glucuronic acid; D-xylose is the most abundant. In this paper, D-xylose was used as the hemicellulose model compound, and it was reacted with chlorine dioxide under simulated bleaching conditions. Gas chromatography-mass spectrometer (GC-MS) was used to determine the reaction products. The effects of pH, temperature, chlorine dioxide dosage, and D-xylose dosage on AOX formation were investigated. The aim of the present work was to appraise the reaction kinetics and mechanism of the reaction of hemicellulose with chlorine dioxide.

EXPERIMENTAL

Materials

D-xylose (purity > 99%) from corn cob was purchased from Alladdin (Shanghai, China). Active carbon adsorption columns (Glass-containers, 180 mL with adapter and insert for quartz-containers 18 × 8 mm) were purchased from Analytik-Jena instrument company (Jena, Germany). Other chemicals were purchased from Alladdin (Shanghai, China). All assay reagents were obtained from Sigma (St. Louis, MO, USA). All chemicals used were of analytical grade.

Reaction Environment

A Multi X2500 AOX analyzer (Jena, Germany) was employed to identify AOX in the bleaching effluent (Yao *et al.* 2017) and was applied for kinetics runs. Solutions of D-xylose were prepared and added to a three-neck flask. A sulfuric acid solution and sodium hydroxide were used to adjust the pH of the solution. Reactions were initiated by mixing D-xylose and chlorine dioxide solutions directly in the three-neck flask. All reactions were conducted at room temperature (25 °C).

Chemical Composition Analysis

AOX was formed by the reaction between D-xylose and chlorine dioxide. AOX may contain more than 300 different organochlorines (Krzmarzick and Novak 2014). To clarify the reaction mechanism of D-xylose and chlorine dioxide, the specific reaction

products were analyzed. The chemical composition of the reaction products and content of D-xylose in the reaction solution were quantified by GC-MS (Agilent 6890-5973, Palo Alto, USA) (Kukkola *et al.* 2006; Singh *et al.* 2008). The basic method and process were described previously (Yao *et al.* 2016). Linear fitting was used to characterize the variation of AOX formation.

RESULTS AND DISCUSSION

Reaction Product Identification

GC-MS was used to determine the content of various compounds in water samples. The reaction conditions were as follows: 10% D-xylose dosage; 2% chlorine dioxide dosage; temperature, 60 °C; time, 60 min; and pH 4. For the reaction solution samples, some peaks were obtained and are listed in Fig. 1. Many peaks appear in the chromatograms at various retention times, indicating that several compounds are contained within the samples. The MS spectrum for each peak was analyzed. The specific compounds in water samples were identified.

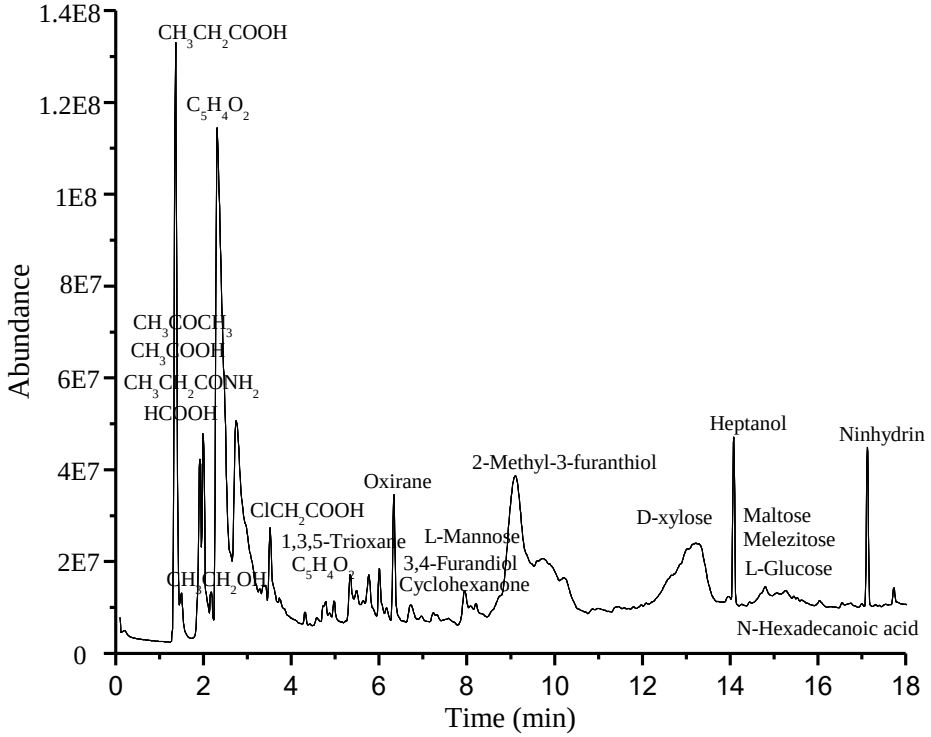

Fig. 1. GC-MS of the reaction solution

The only organochloride compound detected in water samples after the reaction was chloroacetic acid (3.42 min). The sample also contained organic acids. The chemical composition of chlorine dioxide bleaching wastewater was detected by GC-MS; chloroacetic acid was detected. Therefore, the main reaction product was chloroacetic acid. The samples contained organic acids and alkalis, such as propanoic acid (1.36 min and 2.01 min), formic acid (1.92 min), acetic acid (2.09 min, 3.42 min, 9.77 min, 9.88 min, and 10.22 min), ethanol (2.31 min), and erythritol (2.31 min). These organic acids and alkalis were produced by D-xylose

hydrolysis (Kumar *et al.* 2009). Many other esters, ethers, and heterocyclic compounds were detected, such as ethyl ether (1.36 min), ethyl acetate (1.49 min), 2-furanone (2.01 min), 2-propanone (2.18 min), furfural (detected at 2.63 min, 2.74 min, 2.92 min, 3.28 min, and 3.37 min), glyceraldehyde (detected at 4.42 min, 4.51 min, 4.87 min, and 5.15 min), and 1,3,5-trioxane (5.49 min and 5.64 min). These esters, ethers, and heterocyclic compounds were formed by the condensation reactions between organic acids and alkalis (Sonawane *et al.* 2016). In addition, they contain monosaccharides, such as D-arabinose (7.41 min), L-mannose (7.52 min), L-glucose (12.68 min), and xylose (12.74 min). Monosaccharides were formed by the hydrolysis of impurities in the D-xylose samples.

Establishment of Kinetics Model

The mechanism of AOX generation was studied in the reaction of hemicellulose and chlorine dioxide. The reaction process of hemicellulose and chlorine dioxide was studied in a bleaching simulation. The reaction kinetics were presumed to be similar to the delignification and bleaching of chlorine dioxide (Tarvo *et al.* 2010; Brogdon 2012). Based on known chemical reaction kinetics (Nie *et al.* 2014; Ramli and Amin 2016), the kinetic model for AOX formation is shown in Eq. 1,

$$dW / dt = k[H^+]^{\alpha}[ClO_2]^{\beta}X^{\gamma} \quad (1)$$

where dW / dt is the reaction rate, W is the formation of AOX (mg/L), k is the AOX formation rate constant, t is the bleaching time (min), $[H^+]$ is the concentration of hydrogen ion, and X is the amount of consumption of D-xylose in the reaction. The parameters α, β, and γ are the reaction orders of H^+, ClO_2, and D-xylose, respectively. Equation 1 also can be expressed in its logarithmic form, as shown in Eq. 2,

$$\ln(dW/dt) = \ln(k[H^+]^{\alpha}[ClO_2]^{\beta}X^{\gamma}) = \ln k + \alpha\ln[H^+] + \beta\ln[ClO_2] + \gamma\ln[X] \quad (2)$$

where dW / dt is the reaction rate, W is the formation of AOX (mg/L), k is the AOX formation rate constant, H^+ is the concentration of hydrogen ion, and X is the amount of consumption of D-xylose in the reaction. The parameters α, β, and γ are the reaction orders of H^+, ClO_2, and D-xylose, respectively.

Effect of pH on AOX Formation

Chlorine dioxide is a free radical with strong oxidization. Therefore, there are many intermediate mediators in the chlorine dioxide bleaching reaction system, such as ClO_2, $HClO_2$, ClO_2^-, ClO_3^-, HOCl, Cl_2, and Cl^-. The bleaching capacity, however, is reduced by the formation of chlorate. Because the formation of chlorate increases with increasing pH, it is important to control the pH in the reaction. To elucidate the mechanisms affecting chloroacetic acid concentration, tests were performed with the reaction solution by increasing the pH with sulfuric acid and sodium hydroxide. Previous research shows that the bleaching solution pH affects the pulp brightness and yield during chlorine dioxide bleaching. The best pH value of chlorine dioxide bleaching is 3 to 4 (Francis *et al.* 1997; Catalkaya and Kargi 2007). However, there are few reports describing how the joint action of pH and chlorine ions effect AOX concentration in advanced oxidation technologies.

The reaction conditions were as follows: 10% D-xylose dosage; 2.0% chlorine dioxide dosage; temperature, 60 °C; and time, 60 min. The experiments with different pH were selected (1, 2, 3, 4, and 5). Under these conditions, the percentages of the initial D-

xylose was not mineralized, or transformed into other by products. It remained as free sugar. The change in AOX formation with pH is shown in Fig. 2a.

The initial rate of AOX formation at various pH values was obtained by plotting (Table 1), and the results were shown in Fig. 2b. The linear regression is written as Eq. 3,

$$\ln(dW/dt) = \ln(k[ClO_2]^{\beta}X^{\gamma}) + \alpha\ln([H^+]) \quad (3)$$

where dW / dt is the reaction rate, W is the formation of AOX (mg/L), k is the chloroacetic acid concentration rate constant, H^+ is the concentration of hydrogen ion, and X is the amount of consumption of D-xylose in the reaction.

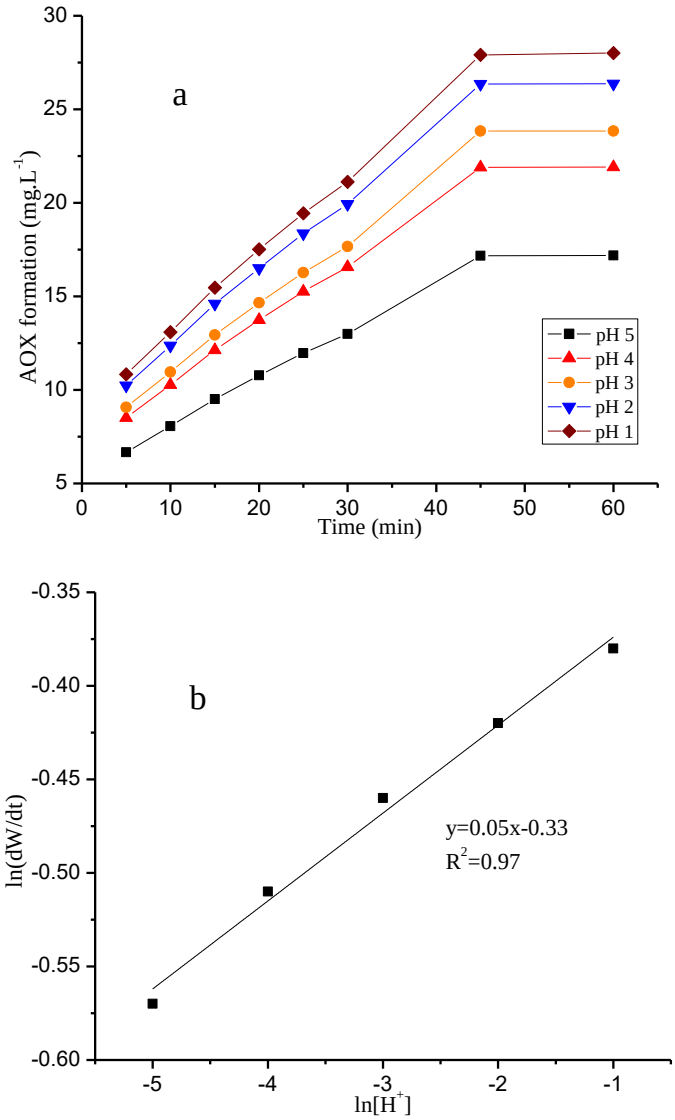

Fig. 2. (a) AOX formation with time under various pH conditions; (b) The linear relationship between ln(d*W*/d*t*) and ln[H⁺]

The determination coefficient R^2 was 0.97, which shows that the fit with the data was excellent. The slope in Fig. 2b was $\alpha = 0.05$. The experimental results showed that the order of H^+ reaction is 0.05, which indicates that H^+ plays a catalytic role in the reaction.

Table 1. Observed Rate Constants on the Basis of pH

pH	Fitting Result	ln(d*W*/d*t*)
1	y = 0.0252x + 0.5343, R^2 = 0.9981	-1.598
2	y = 0.0228x + 0.5041, R^2 = 0.9982	-1.643
3	y = 0.0202x + 0.4380, R^2 = 0.9970	-1.694
4	y = 0.0181x + 0.4193, R^2 = 0.9983	-1.743
5	y = 0.0155x + 0.3288, R^2 = 0.9981	-1.810

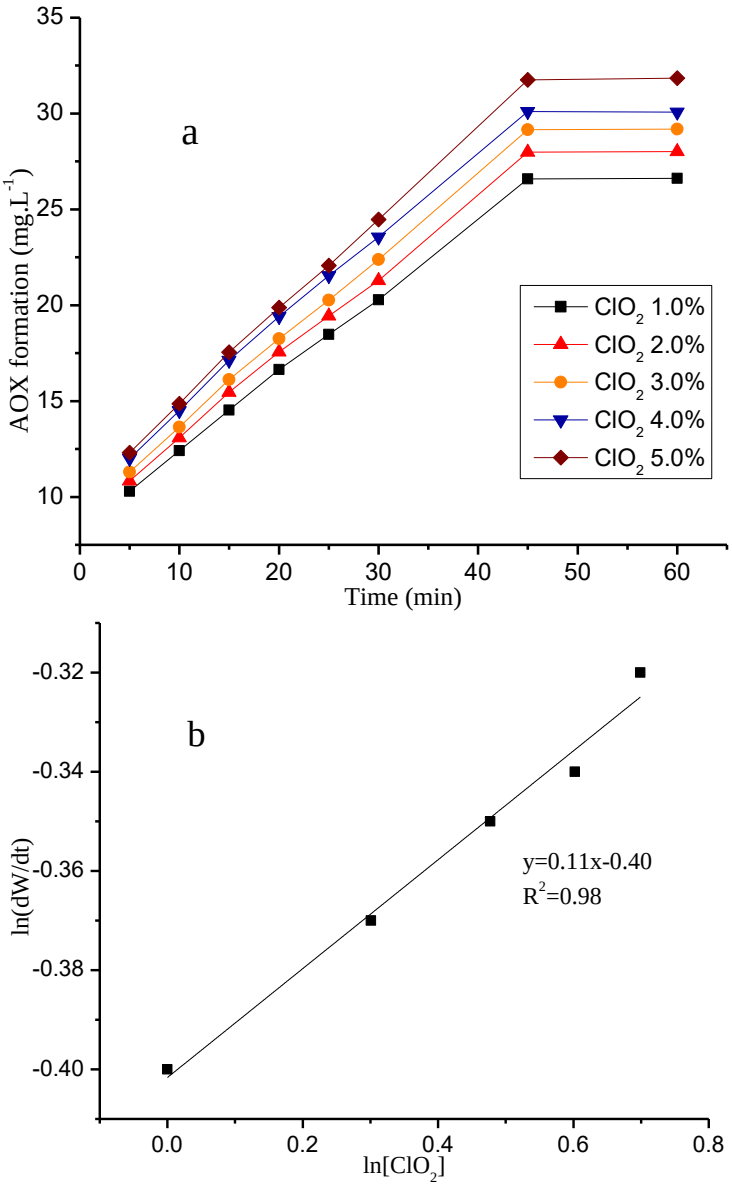

Fig. 3. (a) The AOX formation with time under various ClO_2 dosage; (b) linear relationship between ln(d*W*/d*t*) and ln[ClO_2]

Effect of the ClO_2 Dosage on AOX formation

In this experiment, the dosages of ClO_2 were 1.0%, 2.0%, 3.0%, 4.0%, and 5.0%. The other reaction conditions were as follows: 10% D-xylose dosage, 60 °C, 60 min, and pH 5. The change in chloroacetic acid concentration with time is shown in Fig. 3a.

As shown in Fig. 3a, the change in AOX formation was divided into two stages. AOX formation increased linearly in the initial reaction within 45 min. The variation trend did not change as the ClO_2 dosage increased; it did not extend or shorten. The AOX trended toward saturation as the reaction progressed; it remained unchanged after 45 min. The equilibrium concentrations of AOX formation were 26.51 mg/L, 28.01 mg/L, 29.17 mg/L, 31.01 mg/L, and 31.84 mg/L when the dosages of ClO_2 were 1.0%, 2.0%, 3.0%, 4.0%, and 5.0%, respectively. Although the equilibrium concentration increased as the ClO_2 dosage increased, the rate of growth was relatively stable and did not change with increases in the dosage ClO_2. The growth rate remained unchanged at 5.0%. This was mainly due to the characteristics of the reaction product, chloroacetic acid, as the main medium to produce chloroacetic acid was acetic acid. In fact, acetic acid was generated by D-xylose degradation when D-xylose was added to the reaction solution under acidic conditions, a substitution reaction of chloride ion ensued. The production rate of chloroacetic acid was mainly affected by the supply of acetic acid. The promotion of AOX formation was limited even if the concentration of chloride ions in the solution increased dramatically.

Table 2. Observed Rate Constants on the Basis of ClO_2 Dosage

ClO_2 dosage, %	Fitting Result	lg(dW/dt)
1.0	$y = 0.0242x + 0.5028$, $R^2 = 0.9985$	-1.616
2.0	$y = 0.0260x + 0.5332$, $R^2 = 0.9986$	-1.585
3.0	$y = 0.0271x + 0.5549$, $R^2 = 0.9989$	-1.567
4.0	$y = 0.0281x + 0.5902$, $R^2 = 0.9987$	-1.551
5.0	$y = 0.0288x + 0.6040$, $R^2 = 0.9984$	-1.541

The initial rate of AOX formation at various ClO_2 dosages was calculated by a plotting method (Table 2). The parameter $\ln(dW/dt)$ was the *y*-coordinate, and $\ln[ClO_2]$ was the *x*-coordinate, as shown in Fig. 3b. The linear regression equation was obtained as Eq. 4,

$$\ln(dW/dt) = \ln(k[H^+]^{\alpha}X^{\gamma}) + \beta\ln([ClO_2]) \quad (4)$$

where dW / dt is the reaction rate, W is the formation of AOX (mg/L), k is the AOX formation rate constant, H^+ is the concentration of hydrogen ion, and X is the amount of consumption of D-xylose in the reaction.

The determination coefficient R^2 was 0.98, so the fit with the data was good. The slope in Fig. 3b is $\beta = 0.11$. The order of the ClO_2 reaction is similar to that of H^+ reaction, which is consistent with the conclusions above. The promotion of AOX formation by the addition of chloride ions was limited.

Effect of D-xylose on AOX formation

Excessive acetic acid was provided by 10% D-xylose dosage. To study the effect of D-xylose on AOX formation, the amount of xylose added to the reaction was varied under constant reaction conditions. The saturated D-xylose dosage was determined under 3.0 % ClO_2, 60 °C, 60 min, and pH 5. The results are shown in Fig. 4. The AOX formation was 29.17 mg/L with 4.0 % D-xylose. The formation of AOX did not increase when the D-xylose dosage was increased above 4.0%. Therefore, the saturated dosage of D-xylose was judged to be 4.0 %.

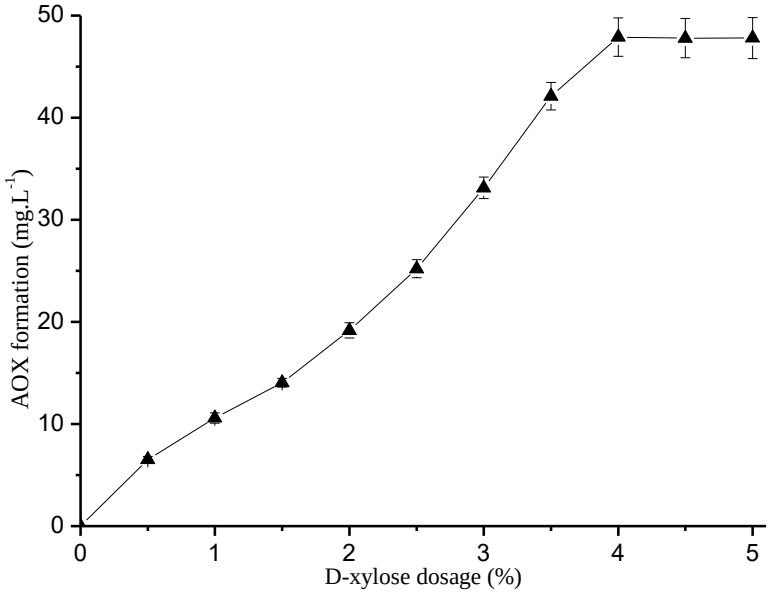

Fig. 4. D-xylose dosage on influence of AOX formation

In this experiment, the dosages of D-xylose were 2.0%, 2.5%, 3.0%, 3.5%, and 4.0%. The other reaction conditions were as follows, 3.0 % ClO_2, 60 °C, 60 min, and pH 5. The change in AOX formation with time is shown in Fig. 5a. The equilibrium concentration of AOX was 14.67 mg/L when the D-xylose dosage was 2.0%, and it increased with increasing D-xylose dosage. The rate of change in the AOX formation was similar when D-xylose 2.5% and 3.0% were used in the reaction. This shows that D-xylose dosage has the most significant effect on AOX formation.

Table 3. Observed Rate Constants on the Basis of D-Xylose Dosage

D-xylose dosage, %	Fitting Result	ln(d*W*/d*t*)
2.0	y = 0.0137x + 0.2735, R^2 = 0.9976	-1.864
2.5	y = 0.0161x + 0.3096, R^2 = 0.9989	-1.794
3.0	y = 0.0194x + 0.3568, R^2 = 0.9987	-1.713
3.5	y = 0.0221x + 0.4322, R^2 = 0.9981	-1.656
4.0	y = 0.0260x + 0.5602, R^2 = 0.9981	-1.585

The initial rate of AOX formation at various D-xylose dosages was calculated using plotting (Table 3). The quantity ln(d*W*/d*t*) was the *y*-coordinate, and ln[X] was the *x*-coordinate; the result is shown in Fig. 5b. The linear regression equation was calculated according to Eq. 5,

$$\ln(dW/dt) = \ln(k[H^+]^{\alpha}[ClO_2]^{\beta}) + \gamma \ln[X] \quad (5)$$

where d*W* / d*t* is the reaction rate, *W* is the formation of AOX (mg/L), *k* is the AOX formation rate constant, $[H^+]$ is the concentration of hydrogen ion, , and *X* is the amount of consumption of D-xylose in the reaction.

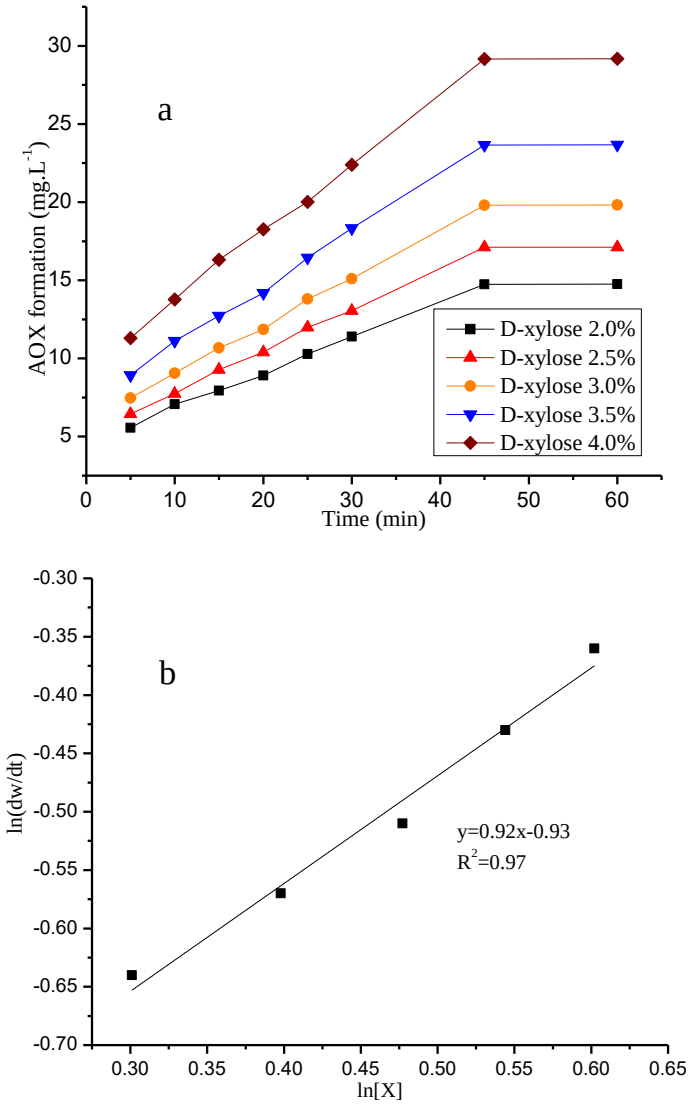

Fig. 5. (a) The AOX formation with time under various D-xylose dosages; (b) Linear relationship between ln(d*W*/d*t*) and ln[X]

The determination coefficient R^2 was 0.97, which shows that the fit with the data was good, and γ was obtained as 0.92. Compared with the reaction order of the H^+ concentration and ClO_2 dosage, the reaction order of the D-xylose dosage was the highest. This result indicated that the limiting factor of the ClO_2 reaction was the amount of D-xylose in the reaction, which has a large influence on the reaction rate. The previous conclusion was verified by the highest reaction order; the production rate of AOX was mainly affected by the supply of acetic acid.

Effect of Temperature on AOX formation

According to the Arrhenius equation, the relationship between temperature and reaction constant *k* was represented by Eq. 6,

$$k = Ae^{-E/RT} \quad (6)$$

$$\ln k = -E/(RT) + \ln A \quad (7)$$

where *A* is the pre-exponential factor, *E* is the reaction activation energy (kJ/mol), *R* is

the gas constant (8.314 J/mol), and *T* is absolute temperature (K). AOX formation at various temperatures (293.15 K, 303.15 K, 313.15 K, 323.15 K, and 333.15 K) with time is shown in Fig. 6a. AOX formation was divided into two stages, one was a rapid growth stage within 45 min and the other was the saturation concentration stage after 45 min. The equilibrium concentration of AOX was 22.50 mg/L at 293.15 K. It increased as the temperature increased and was 24.34 mg/L, 26.01 mg/L, 27.67 mg/L, and 29.17 mg/L at 303.15 K, 313.15 K, 323.15 K, and 333.15 K, respectively. The growth rate of AOX formation was stable. The influence of temperature on the reaction between hemicellulose and chlorine dioxide was limited.

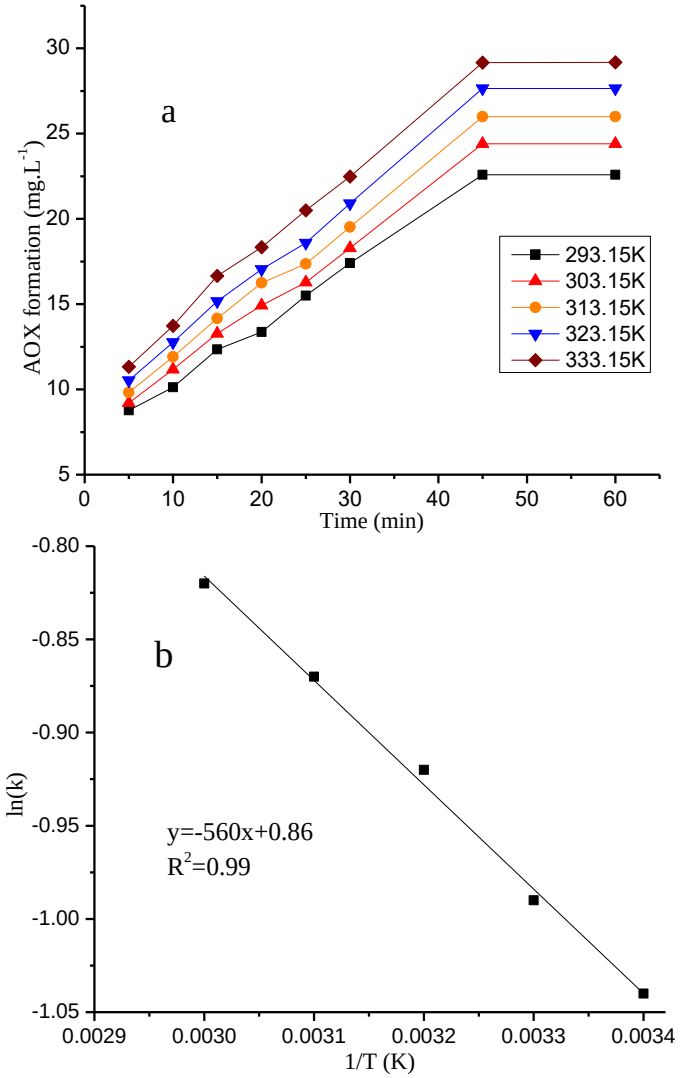

Fig. 6. (a) The AOX formation with time under various temperatures; (b) Linear relationship between ln(*k*) and 1/*T*

Table 4. Observed Rate Constants on the Basis of Temperatures

Temperatures, K	Fitting Result	ln(k)
293.15	y = 0.0209x + 0.4093, R^2 = 0.9967	-3.868
303.15	y = 0.0224x + 0.4429, R^2 = 0.9969	-3.799
313.15	y = 0.0238x + 0.4765, R^2 = 0.9957	-3.738
323.15	y = 0.0252x + 0.5105, R^2 = 0.9973	-3.681
333.15	y = 0.0265x + 0.5677, R^2 = 0.9970	-3.631

Equation 6 also can be expressed in its logarithmic form, as shown in Eq. 7. The initial rate of chloroacetic acid concentration at various temperatures was calculated (Table 4). The parameter ln(k) was the y-coordinate, and 1/T was the x-coordinate. The result is shown in Fig. 6b. The determination coefficient R^2 was 0.99, which shows that the fit with the data was good. The ratio -E/R was -560, which is the slope of the linear equation in Fig. 6b. Therefore, the reaction activation energy E was 4.66 kJ/mol and was very low, indicating that hemicellulose was highly reactive with chlorine dioxide during the chlorine dioxide bleaching process. The intercept of the linear equation, ln(A), was 0.86. Therefore, the pre-exponential factor A was 2.36, and the reaction constant k was $2.36e^{-560/T}$.

Model Accuracy Analysis

The kinetic model was $dW/dt = 2.36e^{-560/T}[H^+]^{0.05}[ClO_2]^{0.11}X^{0.92}$. The AOX concentration from hemicellulose was predicted by the kinetic model during chlorine dioxide bleaching. A comparison between the model predictions and experimental data for the AOX formation is summarized in Fig. 7. Good agreement was obtained between the model predictions and experimental data, with a root mean square error of 2.93%, which lies in the typical range. These results indicate that the kinetic model is a good predictor of AOX concentration from hemicellulose during chlorine dioxide bleaching. The results might open a new door for resolving the major problems of ECF bleaching of pulp.

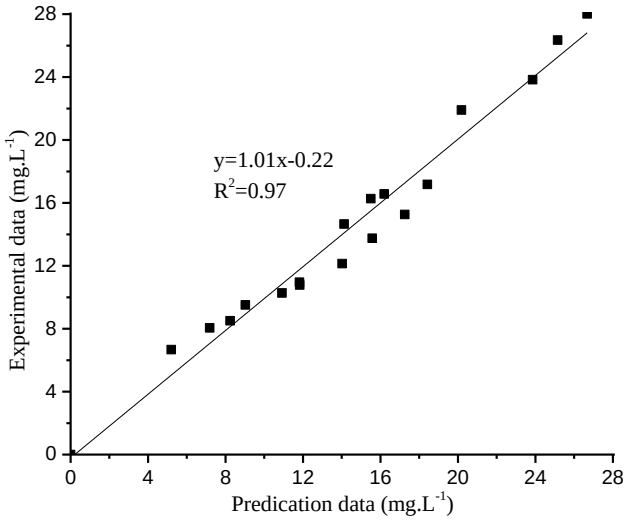

Fig. 7. Experimental and predicted AOX formation

CONCLUSIONS

1. The reaction between D-xylose and chlorine dioxide was studied during bleaching. The final reaction product was chloroacetic acid, a type of AOX.
2. AOX formation was affected by the hemicellulose, and reduced by pre-extraction partial hemicellulose.
3. A kinetic model was developed to investigate the kinetics of hemicellulose conversion to AOX. After evaluating the effects of H^+, ClO_2, D-xylose, and temperature, the kinetics was expressed as $dW/dt = 2.36e^{-560/T}[H^+]^{0.05}[ClO_2]^{0.11}X^{0.92}$. The kinetics was close to first-order, with good agreement between the experimental and modeling data. The activation energies derived from the model were comparatively lower.

ACKNOWLEDGMENTS

This project was sponsored by the National Natural Science Foundation of China (31760192 & 21466004). This project was supported by the Guangxi Natural Science Foundation of China (2016GXNSFBA380234) and the Guangxi Special Funds for Academic and Technical Leaders.

REFERENCES CITED

Baycan, N., Thomanetz, E., and Sengül, F. (2007). "Influence of chloride concentration on the formation of AOX in UV oxidative system," *J. Hazard. Mat.* 143(1-2), 171-176. DOI: 10.1016/j.jhazmat.2006.09.010

Benattar, N., Calais, C., Hamzeh, Y., and Mortha, G. (2007). "Modified ECF bleaching sequences optimizing the use of chlorine dioxide," *Appita J.* 60(2), 150-154.

Bouiri, B., and Amrani, M. (2010). "Elemental chlorine-free bleaching halfa pulp," *Ind. Eng. Chem.* 16(4), 587-592. DOI: 10.1016/j.jiec.2010.03.015

Brogdon, B. (2012). "Stoichiometric model of chlorine dioxide delignification of softwood kraft pulps with oxidant-reinforced extraction effects," *Tappi J.* 11(4), 31-39.

Catalkaya, E. C., and Kargi, F. (2007). "Color, TOC and AOX removals from pulp mill effluent by advanced oxidation processes: A comparative study," *J. Hazard. Mater.* 139(2), 244-253. DOI: 10.1016/j.jhazmat.2006.06.023

Dai, Y., Song, X., Gao, C., He, S., Nie, S., and Qin, C. (2016). "Xylanase-aided chlorine dioxide bleaching of bagasse pulp to reduce AOX formation," *BioResources* 11(2), 3204-3214. DOI: 10.15376/biores.11.2.3204-3214

Fang, C. L., Xiao, D. X., Liu, W. Q., Lou, X. Y., Zhou, J., Wang, Z. H., and Liu, J. S. (2016). "Enhanced AOX accumulation and aquatic toxicity during 2,4,6-trichlorophenol degradation in a Co(II)/peroxymonosulfate/Cl-system," *Chemosphere* 144, 2415-2420. DOI: 10.1016/j.chemosphere.2015.11.030

Francis, D., Turner, P., and Wearing, J. (1997). "AOX reduction of kraft bleach plant effluent by chemical pretreatment—Pilot-scale trials," *Water Res.* 31(10), 2397-2404. DOI: 10.1016/S0043-1354(97)00058-4

Hart, P., and Connell, D. (2008). "Improving chlorine dioxide bleaching efficiency by selecting the optimum pH targets," *Tappi J.* 7(7), 3-11.

Hart, P. W., and Santos, R. B. (2013). "Kraft ECF pulp bleaching: A review of the development and use of techno-economic models to optimize cost, performance, and justify capital expenditures," *Tappi J.* 12(12), 19-29.

Jaacks, L. M., and Staimez, L. R. (2015). "Association of persistent organic pollutants and non-persistent pesticides with diabetes and diabetes-related health outcomes in Asia: A systematic review," *Environ. Int.* 76, 57-70. DOI: 10.1016/j.envint.2014.12.001

Joncourt, M. J., Froment, P., Lachenal, D., and Chirat, C. (2000). "Reduction of AOX formation during chlorine dioxide bleaching," *Tappi J.* 83(1), 144-148.

Krzmarzick, M. J., and Novak, P. J. (2014). "Removal of chlorinated organic compounds during wastewater treatment: Achievements and limits," *Appl. Microbiol. Biotechnol.* 98(14), 6233-6242. DOI: 10.1007/s00253-014-5800-x

Kukkola, J., Knuutinen, J., Paasivirta, J., Herve, S., Pessala, P., and Schultz, E. (2006). "Characterization of high molecular mass material in ECF and TCF bleaching liquors by Py-GC/MS with and without TMAH methylation," *J. Anal. Appl. Pyrol.* 76(1-2), 214-221. DOI: 10.1016/j.jaap.2005.11.006

Kumar, P., Barrett, D. M., Delwiche, M. J., and Stroeve, P. (2009). "Methods for pretreatment of lignocellulosic biomass for efficient hydrolysis and biofuel production," *Ind. Eng. Chem. Res.* 48(8), 3713-3729. DOI: 10.1021/ie801542g

Li, K., Zheng, H., Zhang, H., Zhang, W., Li, K., and Xu, J. (2016). "A novel approach to the fabrication of bleached shellac by totally chlorine-free (TCF) bleaching method," *RSC Advances* 6(60), 55618-55625. DOI: 10.1039/C6RA09132F

Nie, S., Liu, X., Wu, Z., Zhan, L., Yin, G., Yao, S., Song, H., and Wang, S. (2014). "Kinetics study of oxidation of the lignin model compounds by chlorine dioxide," *Chem. Eng. J.* 241(142), 410-417. DOI: 10.1016/j.cej.2013.10.068

Nie, S., Wang, S., Qin, C., Yao, S., Ebonka, J. F., Song, X., and Li, K. (2015). "Removal of hexenuronic acid by xylanase to reduce adsorbable organic halides formation in chlorine dioxide bleaching of bagasse pulp," *Bioresource Technol.* 196, 413-417. DOI: 10.1016/j.biortech.2015.07.115

Nie, S., Zhang, K., Lin, X., Zhang, C., Yan, D., Liang, H., and Wang, S. (2018). "Enzymatic pretreatment for the improvement of dispersion and film properties of cellulose nanofibrils," *Carbohyd. Polym.* 181, 1136-1142. DOI: 10.1016/j.carbpol.2017.11.020

Pei, Y., Wang, S., Qin, C., Su, J., Nie, S., and Song, X. (2016). "Optimization of laccase-aided chlorine dioxide bleaching of bagasse pulp," *BioResources* 11(1), 696-712. DOI: 10.15376/biores.11.1.696-712

Ramli, N. A. S., and Amin, N. A. S. (2016). "Kinetic study of glucose conversion to levulinic acid over Fe/HY zeolite catalyst," *Chem. Eng. J.* 283, 150-159. DOI: 10.1016/j.cej.2015.07.044

Saelee, K., Yingkamhaeng, N., Nimchua, T., and Sukyai, P. (2016). "An environmentally friendly xylanase-assisted pretreatment for cellulose nanofibrils isolation from sugarcane bagasse by high-pressure homogenization," *Ind. Crop Prod.* 82, 149-160. DOI: 10.1016/j.indcrop.2015.11.064

Sharma, A., Thakur, V. V., Shrivastava, A., Jain, R. K., Mathur, R. M., Gupta, R., and Kuhad, R.C. (2014). "Xylanase and laccase based enzymatic kraft pulp

bleaching reduces adsorbable organic halogen (AOX) in bleach effluents: A pilot scale study," *Bioresource Technol.* 169(169), 96-102. DOI: 10.1016/j.biortech.2014.06.066

Singh, S., Chandra, R., Patel, D. K., Reddy, M. M. K., and Rai, V. (2008). "Investigation of the biotransformation of pentachlorophenol and pulp paper mill effluent decolorisation by the bacterial strains in a mixed culture," *Bioresource Technol.* 99(13), 5703-5709. DOI: 10.1016/j.biortech.2007.10.022

Sonawane, S. H., Anniyappan, M., Athar, J., Banerjee, S., and Sikder, A. K. (2016). "Synthesis of bis(propargyl) aromatic esters and ethers: A potential replacement for isocyanate based curators," *RSC Advances* 6(10), 8495-8502. DOI: 10.1039/C5RA25909F

Tarvo, V., Lehtimaa, T., Kuitunen, S., Alopaeus, V., Vuorinen, T., and Aittamaa, J. (2010). "A model for chlorine dioxide delignification of chemical pulp," *J. Wood Chem. Technol.* 30(3), 230-268. DOI: 10.1080/02773810903461476

Wang, L., Zhou, X., Fredimoses, M., Liao, S., and Liu, Y. (2014). "Naturally occurring organoiodines," *RSC Advances* 4(101), 57350-57376. DOI: 10.1039/c4ra09833a

Yao, S., Gao, C., Zhu, H., Zhang, Y., Wang, S., and Qin, C. (2016). "Effects of additives on absorbable organic halide reduction in elemental chlorine-free bleaching of bagasse kraft pulp," *BioResources* 11(1), 996-1006. DOI: 10.15376/biores.11.1.996-1006

Yao, S., Nie, S., Yuan, Y., Wang, S., and Qin, C. (2015). "Efficient extraction of bagasse hemicelluloses and characterization of solid remainder," *Bioresource Technol.* 185, 21-27. DOI: 10.1016/j.biortech.2015.02.052

Yao, S., Nie, S., Zhu, H., Wang, S., Song, X., and Qin, C. (2017). "Extraction of hemicellulose by hot water to reduce adsorbable organic halogen formation in chlorine dioxide bleaching of bagasse pulp," *Ind. Crops Prod.* 96, 178-185. DOI: 10.1016/j.indcrop.2016.11.046

Yeh, R. Y. L., Farre, M. J., Stalter, D., Tang, J. Y. M., Molendijk, J., and Esther, B. I. (2014). "Bioanalytical and chemical evaluation of disinfection by-products in swimming pool water," *Water Res.* 59(4), 172-184. DOI: 10.1016/j.watres.2014.04.002

Yoon, B. H., and Wang, L. J. (2002). "Chlorate reduction in ClO_2 prebleaching by the addition of hypochlorous acid scavengers," *J. Pulp Pap. Sci.* 28(8), 274-279.

Article submitted: April 8, 2018; Peer review completed: May 29, 2018; Revised version received and accepted: May 31, 2018; Published: June 8, 2018.
DOI: 10.15376/biores.13.3.5670-5683